

# Relation between Global and Local EXIT Charts in Hybrid Turbo Codes

Humberto V. Beltrão Neto and Werner Henkel

Jacobs University Bremen

Campus Ring 1

D-28759 Bremen, Germany

Email: {h.beltrao, w.henkel}@jacobs-university.de

**Abstract**—This paper describes the relation between the two different kinds of EXIT charts that arise in the analysis of a hybrid concatenated turbo coding scheme used for achieving unequal error protection capabilities. From this analysis, it is shown that both kinds of charts can be used for analyzing the iterative decoding procedure of such hybrid concatenated codes. Finally, it is shown that the study of the hybrid turbo codes can be reduced to the study of the component serial concatenated codes.

## I. INTRODUCTION

Turbo codes [1] were originally defined as parallel concatenated codes (PCCs), i.e., a parallel concatenation of two binary convolutional codes with the parallel branches separated by one interleaver of appropriate size, decoded by an iterative decoding algorithm. Later, Benedetto et al. [2] introduced a serial concatenation of interleaved codes. Those serially concatenated codes (SCCs) in general exhibit lower error floors than PCCs, but SCCs usually converge further away from channel capacity. A further form of concatenated code, hybrid concatenated codes (HCCs), consists of a combination of parallel and serial concatenation, offering the opportunity to exploit the advantages of parallel and serially concatenated codes. There are several different hybrid concatenated structures proposed in literature, e.g., [3], [4]. In this paper, we study the hybrid scheme proposed in [5], which is depicted in Fig. 1. This kind of concatenation consists of a parallel concatenation of two serially concatenated interleaved codes and arises in the context of turbo coding schemes with unequal error protection (UEP) properties.

In [6], the authors showed that a pruning procedure can be employed for adapting the rate and distance for different protection levels in UEP turbo codes. Pruning can simply be accomplished by a concatenation of a mother code and a pruning code which leads to a selection of only some paths in the decoding trellis. In Fig. 1, the codes  $G_{11}$  and  $G_{21}$  can be referred to as the pruning codes and  $G_{12}$  and  $G_{22}$  as the mother codes of such a UEP scheme. As a tool for investigating the iterative decoding behavior of this hybrid concatenation, we make use of ten Brink's EXIT charts [7]. We can however define two different EXIT charts for the studied concatenation. The first one, which we call local EXIT chart, examines the iterative decoding behavior of the serial concatenated codes. The second one, which we call global EXIT chart, deals with

the exchange of information between each parallel branch during the decoding procedure. Our objective is to derive the relation between these different charts, showing that the design of hybrid turbo codes can, by means of the local EXIT chart, be reduced to that of serially interleaved concatenated codes.

This paper is organized as follows. The system model of the encoding and decoding of hybrid concatenated codes is reviewed in Section II. In Section III, we analyze iterative decoding by means of the global and local EXIT charts. The relation between those charts is derived in Section IV. The construction of the local EXIT chart by means of the information transfer characteristic curve for the outer and inner decoders of the serial concatenation is analyzed in Section V. Finally, conclusions are summarized in Section VI.

## II. HYBRID TURBO CODES

Hybrid turbo codes [5] are constructed by means of a parallel concatenation of serially concatenated codes. Figure 1 shows the corresponding encoder system. In the following, all component codes are assumed to be recursive systematic convolutional codes (RSC). The interleavers in the upper and lower branch are denoted as  $\Pi_1$  and  $\Pi_2$ , respectively. Since the output of each parallel branch is systematic, the information bits only have to be transmitted once. The example codes used in this paper are given by

$$G_{11} = G_{21} = \left( 1 \quad \frac{D^2}{1+D+D^2} \right) \quad (1)$$

and

$$G_{12} = G_{22} = \left( \begin{array}{cc} 1 & 0 \\ 0 & 1 \end{array} \frac{1+D+D^2}{1+D^2} \right) \quad (2)$$

In this example, the outer codes have rates  $R_{11} = R_{21} = 1/2$  and the inner codes rates are  $R_{12} = R_{22} = 2/3$ . The systematic coded bit stream is composed as follows

$$\mathbf{c} = (c_{1,1}(1) \ c_{1,2}(1) \ c_{1,3}(1) \ c_{2,2}(1) \ c_{2,3}(1) \\ c_{1,1}(2) \ c_{1,2}(2) \ c_{1,3}(2) \ c_{2,2}(2) \ c_{2,3}(2) \ \dots),$$

where  $c_{1,1}(1) = u(1)$ ,  $c_{1,1}(2) = u(2)$  and so on. Note that  $c_{2,1}(\cdot)$  is not transmitted since we do not want to transmit the systematic information twice. Thus, the overall rate of our example code is  $R = 1/5$ . The decoding operation of such codes is divided in a local decoding operation corresponding to each parallel branch, and a global decoding operation where

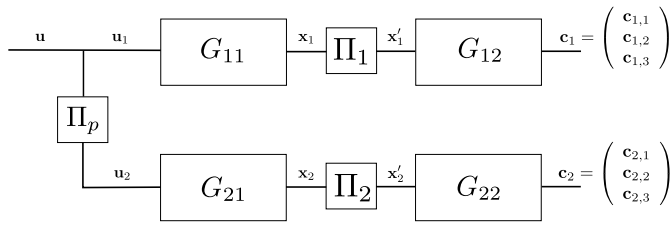


Fig. 1. Encoder structure of a hybrid turbo code.

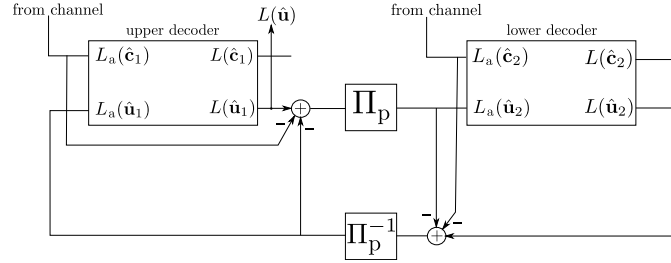


Fig. 2. Decoder structure of the parallel concatenation present in the hybrid turbo code.

the parallel branches exchange extrinsic information between them. We will first explain the local decoding operation and then show how to connect the partial results for each parallel branch to form the global decoding system. As component decoders we assume *a posteriori* decoders (APP decoders, e.g., BCJR, logMAP) which have two inputs and two outputs in form of log-likelihood ratios ( $L$ -values).

#### A. Iterative decoding of the parallel concatenated codes

Both decoders of the parallel concatenation receive as first input the channel observation (intrinsic information). As this information can be interpreted as *a priori* information concerning the coded stream, we will call it  $L_a(\hat{c}_j)$  where the indices  $j = 1$  and  $j = 2$  refer to the upper and lower branch, respectively. The second input represents the *a priori* information concerning the uncoded bit streams denoted by  $L_a(\hat{u}_j)$ . The decoder outputs two  $L$ -values corresponding to the coded and uncoded bit streams denoted by  $L(\hat{c}_j)$  and  $L(\hat{u}_j)$ , respectively. Figure 2 shows the corresponding system. For systematic codes, the decoder outputs are composed of the two *a priori* values and some extrinsic information gained by the decoding process. In order to avoid statistical dependencies, the two decoders only exchange the extrinsic  $L$ -values corresponding to the uncoded bit stream  $L_e(\hat{u}_j) = L(\hat{u}_j) - L_a(\hat{u}_j) - L_a(\hat{c}_j)$ .

#### B. Iterative decoding of the serially concatenated codes

For a serial concatenation with interleaver  $\Pi_j$ , let  $\mathbf{u}_j$  and  $\mathbf{x}_j$  be the input and output of the outer encoder, and let  $\mathbf{x}'_j$  and  $\mathbf{c}_j$  be the input and output of the inner encoder, respectively. For each iteration, the inner decoder receives the intrinsic information  $L_a(\hat{c}_j)$  and the *a priori* knowledge on the inner information bits  $L_a(\hat{x}'_j)$ . Accordingly, the inner decoder outputs two  $L$ -values corresponding to the coded and uncoded bit streams denoted by  $L(\hat{c}_j)$  and  $L(\hat{x}'_j)$ , respectively. The difference  $L(\hat{x}'_j) - L_a(\hat{x}'_j)$ , which combines extrinsic and

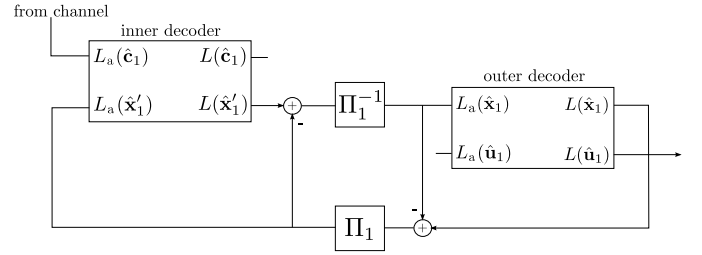


Fig. 3. Decoder structure of the upper branch for the hybrid turbo code

channel information, is then passed through a bit deinterleaver to become the *a priori* input  $L_a(\hat{x}_j)$  of the outer decoder. The outer decoder feeds back extrinsic information  $L_e(\hat{x}_j) = L(\hat{x}_j) - L_a(\hat{x}_j)$  which becomes the *a priori* knowledge  $L_a(\hat{x}'_j)$  for the inner decoder. It is worth noting that the *a priori* information concerning the uncoded input of the outer decoder is zero all the time, since there is no information from this side of the decoder<sup>1</sup>. Furthermore, the outer decoder does not pass information corresponding to the uncoded but to the coded bits to the inner decoder, since the (interleaved) coded output of the outer encoder corresponds to the uncoded input of the inner encoder. The decoder structure of the upper branch ( $j = 1$ ) is depicted in Fig. 3.

#### C. The hybrid turbo code decoding procedure

Once we know how the serial and parallel decoding is performed, we are able to describe the decoding procedure of the whole system. At first, the channel provides information about the outputs of the two inner encoders, that is,  $L_a(\hat{c}_1)$  and  $L_a(\hat{c}_2)$ . We assume the upper branch to be decoded first. Thus, the upper inner decoder calculates the estimated vector of  $L$ -values  $L(\hat{x}'_1)$  subtracts its *a priori*  $L$ -values  $L_a(\hat{x}'_1)$  and then passes it to the outer decoder (note that for the first iteration  $L_a(\hat{x}'_1) = 0$ ). The outer decoder receives  $L_a(\hat{x}_1) = \Pi_1^{-1}(L(\hat{x}'_1) - L_a(\hat{x}'_1))$ , calculates its estimated  $L$ -values  $L(\hat{x}_1)$ , and then passes the extrinsic information  $L_e(\hat{x}_1) = L(\hat{x}_1) - L_a(\hat{x}_1)$  to the upper inner decoder. This procedure is performed for a certain number iterations  $n_{it,1}$ . At the end of these iterations, the upper branch calculates the extrinsic information regarding the information bits  $L_e(\hat{u}_1) = L(\hat{u}_1) - L_a(\hat{u}_1) - L_a(\hat{c}_1)$  and passes it on to the lower branch. Note that  $L_a(\hat{u}_1) = 0$  is zero when this value is calculated for the first time. The decoding of the lower branch starts with the activation of the outer decoder, which receives *a priori* information from the upper branch  $L_a(\hat{u}_2) = \Pi_p(L_e(\hat{u}_1))$  and from the channel  $L_a(\hat{x}_2)$ . Note that, since the inner encoder is systematic, the channel information regarding the output of the outer encoder is the systematic part of the inner encoder output, thus it can be passed on to the outer decoder without activation of the inner decoder. The outer decoder computes the values  $L(\hat{x}_2)$  and passes the extrinsic

<sup>1</sup>This is assumed here because we are dealing solely with the decoding procedure of one parallel branch. When dealing with the whole hybrid system,  $L_a(\hat{x}'_j)$  will vary since it is the information exchanged between the parallel branches.



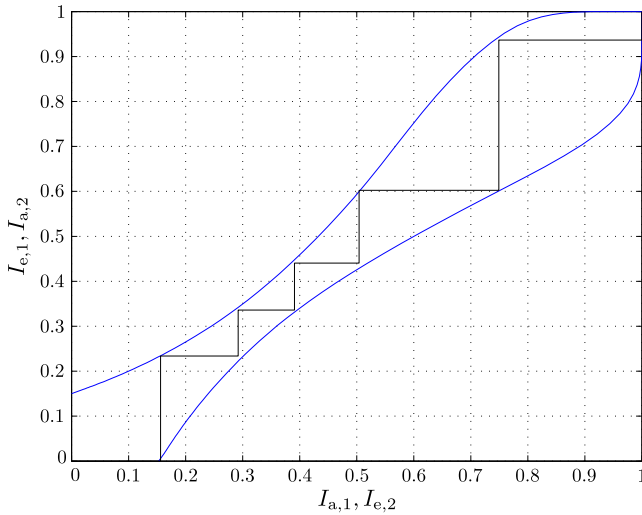


Fig. 6. Global EXIT chart with decoding trajectory for the example hybrid turbo code with  $n_{it,1} = n_{it,2} = 2$  and  $E_b/N_0 = 1$  dB.

decoder in a parallel concatenation. The global EXIT chart depicts the mutual information concerning the *a priori* values  $L_a(\hat{\mathbf{u}}_j)$  and the extrinsic values  $L_e(\hat{\mathbf{u}}_j) = L(\hat{\mathbf{u}}_j) - L_a(\hat{\mathbf{u}}_j) - L_a(\hat{\mathbf{c}}_j)$ . The global EXIT chart for  $E_b/N_0 = 1$  dB is shown in Fig. 6.

Note that due to the different code rates for the global and local systems, the corresponding local EXIT chart is depicted in Fig. 5 for  $E_b/N_0 = -1.22$  dB, i.e.,

$$\frac{E_b}{N_0} \Big|_{dB, R=1/5} = \frac{E_b}{N_0} \Big|_{dB, R=1/3} + 10 \log_{10} \frac{5}{3}. \quad (3)$$

As expected from the analysis of the corresponding local EXIT chart depicted in Fig. 5, the iterative decoding converges.

#### IV. RELATION BETWEEN LOCAL AND GLOBAL EXIT CHARTS

The analysis of both local and global EXIT charts provides a good insight into the iterative decoding procedure. Since they lead to the same conclusion about the decoder convergence, a mathematical relation between them is to be expected. The derivation of this relation is the subject of the present section.

The local EXIT charts depict the relation between the *a priori* and extrinsic information concerning the codewords of the outer decoder, i.e., it shows the relation between  $I(\mathbf{x}; L_a(\hat{\mathbf{x}})) = I_{a,o}(\hat{\mathbf{x}})$  and  $I(\mathbf{x}; L_e(\hat{\mathbf{x}})) = I_{e,o}(\hat{\mathbf{x}})$ . Note that for finitely long sequences, the mutual information between some data sequence  $\mathbf{x}$  and the corresponding  $L$ -values  $L(\hat{\mathbf{x}})$  is given by

$$I = I(\mathbf{x}; L(\hat{\mathbf{x}})) = E\{1 - \log_2(1 + e^{-x_l \cdot L(\hat{x}_l)})\}. \quad (4)$$

The global EXIT chart, instead, plots the mutual information concerning the *a priori* and extrinsic values regarding the information bits, i.e.,  $I(\mathbf{u}; L_a(\hat{\mathbf{u}})) = I_{a,j}(\hat{\mathbf{u}})$  and  $I(\mathbf{u}; L_e(\hat{\mathbf{u}})) = I_{e,j}(\hat{\mathbf{u}})$  where  $j = 1$  (upper branch), 2 (lower branch).

In the local EXIT charts we should now focus on the points where  $I_{a,o}(\hat{\mathbf{x}}) = 0$ , i.e., the points where the *a priori* information regarding the output bits of the outer encoder is zero. In this situation, all the knowledge that the outer decoder has about  $\hat{\mathbf{x}}$  comes from the information regarding  $\hat{\mathbf{u}}$  provided by the other branch. Since the code is systematic, it is not difficult to see that

$$I_{e,o}(\hat{\mathbf{x}}) = R_o \cdot I_{a,j}(\hat{\mathbf{u}}), \quad (5)$$

where  $R_o$  is the rate of the outer code and  $j = 1$  or 2 depending whether the upper or lower decoder was activated in the corresponding local decoding, respectively. Equation (5) relates two quantities that are depicted in different EXIT charts, thus it can be used to link both representations. On the one hand, from the local EXIT chart, we will be able to calculate the global decoding trajectory from the points of zero ordinate ( $I_{a,o}(\hat{\mathbf{x}}) = 0$ ), since at these points, all the knowledge that the outer decoder has about  $\hat{\mathbf{x}}$  comes from the information regarding  $\hat{\mathbf{u}}$ . Then, using Eq. (5), we can compute the corresponding  $I_{a,j}(\hat{\mathbf{u}})$ . On the other hand, by directly evaluating from the global EXIT chart where the decoding trajectory and the transfer curve of the active branch meet, one can compute the points of the local EXIT chart where  $I_{a,o}(\hat{\mathbf{x}}) = 0$ . This situation is shown in Fig. 7 for the local and global EXIT charts depicted in Fig. 5 and Fig. 6. Note that since the  $R_o = 0.5$ ,  $I_{e,o}(\hat{\mathbf{x}}) = 0.5 \cdot I_{a,j}(\hat{\mathbf{u}})$  where  $j = 1$  for the upper branch (dashed arrows) and  $j = 2$  for the lower one (solid arrows).

In Fig. 8, we see the local EXIT chart for  $E_b/N_0 = -1.77$  dB. From this chart, we can observe that the decoding will not converge for this SNR due to the intersection between the transfer curves of the inner and outer decoder. It is worth noting that, in this example, the more local iterations are performed, the closer the transfer curves of the outer decoder lie to each other. This reflects the fact that there is no further gain of information about  $\hat{\mathbf{u}}$ . This is depicted in the corresponding global EXIT chart of Fig. 9 when the transfer curves of each branch intersect. Note that, as stated in Eq. (5), the point to where the transfer curves converge is exactly half of the ordinate of the point where the transfer curves of the global EXIT chart intersect.

#### V. CONSTRUCTION OF THE LOCAL EXIT CHART FROM THE TRANSFER CHARACTERISTIC OF THE INNER AND OUTER CODES

We still need to show how to construct the local EXIT charts from the transfer characteristic of the inner and outer codes. Doing this, reduces the design of good hybrid turbo codes to the well known design of serially concatenated convolutional codes [9]. In order to construct the whole local EXIT chart, we must be able to compute the *a priori* information regarding the message bits ( $I_a(\hat{\mathbf{u}})$ ) since for each  $I_a(\hat{\mathbf{u}})$  (that remains constant during each local decoding operation) we will have a different transfer curve for the outer decoder.

The problem can be formulated as follows: given  $I_{a,o}(\hat{\mathbf{x}})$ ,  $I_{e,o}(\hat{\mathbf{x}})$ , and  $I_a(\hat{\mathbf{u}})$ , compute  $I_e(\hat{\mathbf{u}})$ . It should be clear that

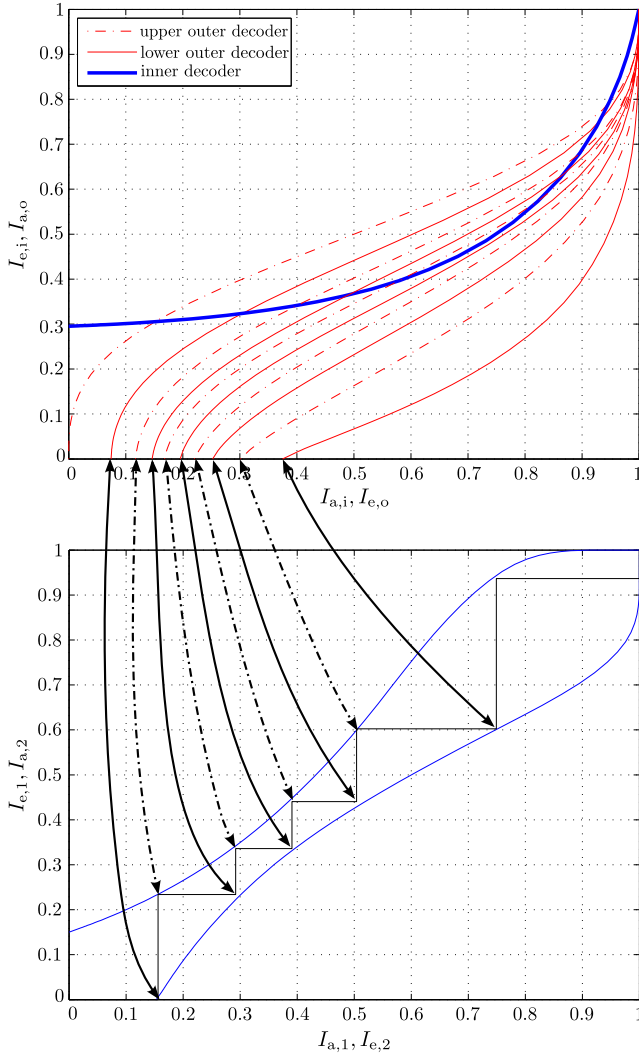


Fig. 7. Depiction of the relation between the points  $I_{a,o}(\hat{\mathbf{x}}) = 0$  in the local EXIT chart and the global decoding trajectory for the example hybrid turbo code. Charts constructed for  $E_b/N_0 = 1$  dB (related to the global system).

$I_{a,o}(\hat{\mathbf{x}})$  and  $I_{e,o}(\hat{\mathbf{x}})$  can be evaluated from the EXIT chart of the serial concatenation for a given  $I_a(\hat{\mathbf{u}})$ . Note that  $I_a(\hat{\mathbf{u}})$  is calculated recursively, that is,  $I_a(\hat{\mathbf{u}})_2^{it,g} = I_e(\hat{\mathbf{u}})_1^{it,g}$  for  $it, g \geq 0$ ,  $I_a(\hat{\mathbf{u}})_1^{it,g} = I_e(\hat{\mathbf{u}})_2^{it,g-1}$  for  $it, g > 0$ , and  $I_a(\hat{\mathbf{u}})_1^0 = 0$  where  $it, g$  stands for the current global iteration<sup>2</sup> (subscripts 1 and 2 stand for upper and lower branch, respectively).

The soft output of the outer decoder concerning the information bits can be written as

$$L_e(\hat{\mathbf{u}}) = L(\hat{\mathbf{u}}) - L_a(\hat{\mathbf{u}}) - L_{ch}(\hat{\mathbf{u}}). \quad (6)$$

where  $L_{ch}(\hat{\mathbf{u}})$  is the intrinsic information concerning the uncoded bits. As indicated by simulations, we assume the random variables involved to have a symmetric Gaussian distribution. Under the Gaussian assumption and assuming independence between the random variables involved, we can

<sup>2</sup>Remember that we are assuming the upper branch to be decoded first.

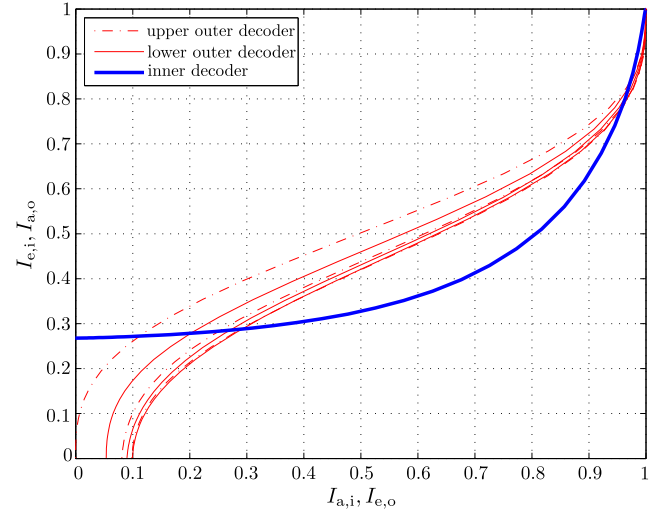


Fig. 8. Local EXIT chart for the example hybrid turbo code for  $E_b/N_0 = 0.5$  dB (relating to the the whole system). Local decoders do not converge for this SNR.

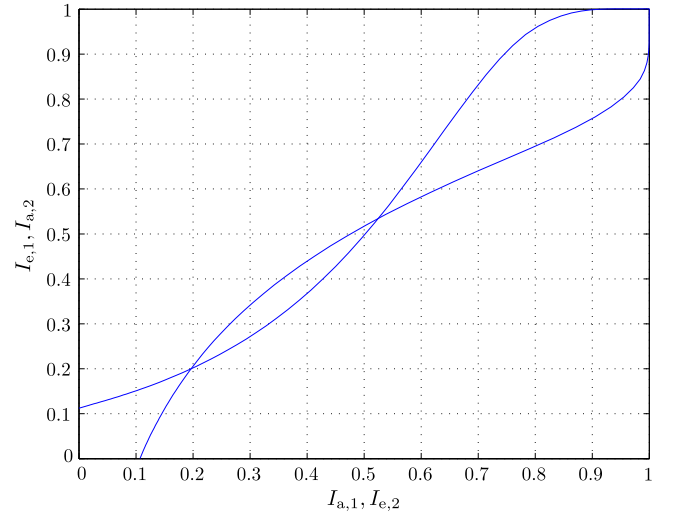


Fig. 9. Global EXIT chart of a hybrid turbo code for  $E_b/N_0 = 0.5$  dB.

write

$$\sigma_e^2 = \sigma_u^2 - \sigma_a^2 - \sigma_{ch}^2. \quad (7)$$

The bitwise mutual information of Gaussian log-likelihood ratio distributions with variance  $\sigma^2$  and mean  $\mu = \sigma^2/2$  (symmetry condition) is given by the  $J(\cdot)$  function with [8]

$$J(\sigma) = 1 - \int_{-\infty}^{\infty} \frac{e^{-\frac{(\xi - \sigma^2/2)^2}{2\sigma^2}}}{\sqrt{2\pi}\sigma} \cdot \log_2[1 + e^{-\xi}] d\xi. \quad (8)$$

The function  $J(\sigma)$  cannot be expressed in closed form, but it is monotonically increasing and thus invertible. According to [10] it can be closely approximated by

$$J(\sigma) \approx (1 - 2^{-H_1 \sigma^2 H_2})^{H_3}, \quad (9)$$

$$J^{-1}(I) \approx \left(-\frac{1}{H_1} \log_2(1 - I^{\frac{1}{H_3}})\right)^{\frac{1}{2H_2}}, \quad (10)$$

with  $H_1 = 0.3073$ ,  $H_2 = 0.8935$ , and  $H_3 = 1.1064$ . The variances  $\sigma_a^2$ ,  $\sigma_{ch}^2$ , and  $\sigma_u^2$  can be calculated inverting the  $J(\cdot)$  function

$$\sigma_a^2 \approx J^{-1}(I_a(\hat{\mathbf{u}}))^2, \sigma_{ch}^2 \approx J^{-1}(I_{ch}(\hat{\mathbf{u}}))^2, \sigma_u^2 \approx J^{-1}(I(\hat{\mathbf{u}}))^2,$$

where  $I_{ch}(\hat{\mathbf{u}}) = I(\mathbf{u}; L_{ch}(\hat{\mathbf{u}}))$  and  $I(\hat{\mathbf{u}}) = I(\mathbf{u}; L(\hat{\mathbf{u}}))$ . Note that  $I_{ch}(\hat{\mathbf{u}})$  can be inferred from the local EXIT chart from the point where the inner decoder information transfer curve intersects the ordinate axis.  $I(\hat{\mathbf{u}})$  can be calculated from the local EXIT chart in the following way.

Since  $L(\hat{\mathbf{x}}) = L_e(\hat{\mathbf{x}}) + L_a(\hat{\mathbf{x}})$ , and assuming that  $L_e(\hat{\mathbf{x}})$  and  $L_a(\hat{\mathbf{x}})$  are independent Gaussian distributed variables, we can write

$$\sigma_x^2 = \sigma_e^2 + \sigma_a^2, \quad (11)$$

and thus compute  $I(\mathbf{x}; L(\hat{\mathbf{x}})) = I(\hat{\mathbf{x}}) = J(\sigma_x)$ . Finally, note that  $I(\hat{\mathbf{x}})$  contains information regarding both parity and information bits. By means of Eq. (4), we can write

$$I(\hat{\mathbf{x}}) = I(\hat{\mathbf{u}}) \cdot R_o + I(\hat{\mathbf{p}}) \cdot (1 - R_o), \quad (12)$$

where  $R_o$  is the rate of the outer code and  $I(\hat{\mathbf{p}})$  is the information regarding the parity-check bits. Assuming that the  $L$ -values carry approximately the same amount of information for every bit we can say that  $I(\hat{\mathbf{u}}) \approx I(\hat{\mathbf{p}})$  and then

$$I(\hat{\mathbf{u}}) \approx I(\hat{\mathbf{x}}). \quad (13)$$

Note that Eq. (5) can also be derived from (12) by noticing that in the points of the local EXIT chart where  $I_{a,o}(\hat{\mathbf{x}}) = 0$ , the information about the parity bits equals zero, that is,  $I(\hat{\mathbf{p}}) = 0$ . By means of Eqs. (7), (8), (11), and (13), we can compute the extrinsic information regarding the message bits  $I_e(\hat{\mathbf{u}})$  and then compute the transfer curve of the outer decoder when  $I_a(\hat{\mathbf{u}}) \neq 0$  thus deriving the complete local EXIT chart. With the local EXIT chart and Eq. (5), we are able to predict the convergence behavior of the global system without the need of constructing the whole global EXIT chart. That is, the convergence of the system may be predicted locally by analyzing the local EXIT charts.

## VI. CONCLUSION

We derived the construction of local EXIT charts for a hybrid concatenation of convolutional codes that we named hybrid turbo codes and showed the relation between the latter and the global EXIT charts. It was shown that for points in the local EXIT charts where the *a priori* information of the outer decoder regarding the code bits is equal to zero ( $I_{a,o}(\hat{\mathbf{x}}) = 0$ ), a simple relation between local and global EXIT charts is derived, i.e., for such points  $I_{e,o}(\hat{\mathbf{x}}) = R_o \cdot I_{a,j}(\hat{\mathbf{u}})$  where  $R_o$  is the rate of the outer code and  $j = 1$  or  $2$  depending whether the upper or lower decoder was activated in the parallel concatenation. This enables us to check the convergence behavior of the global system through the local EXIT chart.

We also showed that for systematic encoding, the bitwise mutual information regarding the codeword and its received  $L$ -value ( $I(\mathbf{x}; L(\hat{\mathbf{x}})) = I(\hat{\mathbf{x}})$ ) can be split into the information related to the parity and the information bits. Based on this, and on the independence of channel, *a priori*, and extrinsic information, we derived a relation that enabled us to compute the *a priori* information regarding the message bits ( $I(\hat{\mathbf{u}})$ ) at the end of the local iterations what enables us to construct the complete local EXIT chart for a given code from the transfer characteristics of the outer and inner decoder of the serial concatenation. This reduces the analysis of the global system to the study of a serial concatenated code, since the convergence behavior of the global system can be predicted from the local EXIT chart.

## ACKNOWLEDGMENTS

The authors would like to thank Neele von Deetzen for providing simulation programs and Prof. Valdemar C. da Rocha Jr. for helpful discussions and suggestions. This work is funded by the German National Science Foundation (DFG).

## REFERENCES

- [1] C. Berrou, A. Glavieux and P. Thitimajshima, "Near Shannon limit error-correcting coding and decoding: turbo codes," *Proc. IEEE International Conference on Communication (ICC)*, May 1993, Geneva, Switzerland, pp. 1064-1070.
- [2] S. Benedetto, D. Divsalar, G. Montorsi and F. Pollara, "Serial concatenation of interleaved codes: performance analysis, design, and iterative decoding," *IEEE Transactions on Information Theory*, vol. 44, no. 3, pp. 909-926, May 1998.
- [3] D. Divsalar and F. Pollara, "Serial and hybrid concatenated codes with applications," in *Proc. Int. Symp. on Turbo Codes and Related Topics*, Brest, France, Sept. 1997, pp. 80-87.
- [4] H. Gonzalez, C. Berrou, and S. Kerouadan, "Serial/parallel turbo codes for low error rates," in *IEEE Military Commun. Conf. (MILCOM'05)*, vol. 1, pp. 346-349, 2004.
- [5] N. von Deetzen and W. Henkel, "Decoder scheduling of hybrid turbo codes," *IEEE International Symposium on Information Theory*, July 2006, Seattle, USA.
- [6] W. Henkel and N. von Deetzen, "Path pruning for unequal error protection," *International Zurich Seminar on Communications*, February 2006, Zurich, Switzerland.
- [7] S. ten Brink, "Convergence of iterative decoding," *Electronics Letters*, vol. 35, no. 10, pp. 806-808, May 1999.
- [8] S. ten Brink, "Convergence behavior of iteratively decoded parallel concatenated codes," *IEEE Trans. on Communications*, vol. 49, no. 10, pp. 1727-1737, Oct. 2001.
- [9] S. ten Brink, "Code characteristic matching for iterative decoding of serially concatenated codes," *Annals of Telecommunications*, vol. 56, no. 7-8, pp. 394-408, Jul. 2001.
- [10] F. Brännström, "Convergence analysis and design of multiple concatenated codes," Ph.D. dissertation, Chalmers Univ. Technology, Göteborg, Sweden, Mar. 2004.